Seismological Research Letters

The influence of cumulative intensity on macroseismic source parameters: the case of 2016-2017 and 1703 seismic sequences (Central Italy)

--Manuscript Draft--

Manuscript Number:	SRL-D-22-00038R4
Full Title:	The influence of cumulative intensity on macroseismic source parameters: the case of 2016-2017 and 1703 seismic sequences (Central Italy)
Article Type:	Article - Regular Section
Corresponding Author:	Laura Graziani Istituto Nazionale di Geofisica e Vulcanologia Rome, ITALY
Corresponding Author Secondary Information:	
Corresponding Author's Institution:	Istituto Nazionale di Geofisica e Vulcanologia
Corresponding Author's Secondary Institution:	
First Author:	Laura Graziani
First Author Secondary Information:	
Order of Authors:	Laura Graziani
	Andrea Rovida
	Andrea Tertulliani
Order of Authors Secondary Information:	
Manuscript Region of Origin:	ITALY
Abstract:	The macroseismic source parameters of earthquakes occurring within a sequence are strongly influenced by cumulative damage effects. When we deal with historical seismic sequences, in addition to the cumulative intensities, other intrinsic uncertainties due to the scarcity and indeterminacy of sources come into play. These issues imply that the parameterizations of the single shocks within a historical seismic sequence are not univocal and that all the uncertainties that are addressed when assessing macroseismic intensity should be carefully considered in the parameter estimation. In the light of these considerations, we performed some tests on the 2016-2017 and 1703 seismic sequences, which occurred in the same area in Central Italy, to compute the macroseismic source parameters by means of two independent methods. Results show that the cumulative effects arising from multiple damaging shocks can cause biases in the intensity assessments, which affect the computed magnitude and epicentral locations. To reduce bias in macroseismic intensities due to cumulative damage, we illustrate a simple procedure, called Cumulative Intensity Subtraction (CIS), which consists in discarding the localities strongly damaged by the early earthquakes of a sequence from the intensity distributions used for computing the macroseismic source parameters of the subsequent shocks. The outcomes show that, for the 2016 seismic sequence, the CIS approach provides locations in agreement with the instrumental epicenters and with the causative faults. For the 1703 sequence the CIS approach along with explicit accounting for the indeterminacy in intensity assignments give a range of equally plausible solutions. The CIS represents an exploration of a simple strategy that stems from an attempt to give significance to macroseismic intensity in the presence of cumulative damage.
Suggested Reviewers:	Paolo Galli paolo.galli@protezionecivile.it
	Ina Cecic ina.cecic@gov.si
Opposed Reviewers:	

The influence of cumulative intensity on macroseismic source parameters: the case of 2016-2017 and 1703 seismic sequences (Central Italy)

L. Graziani[(1)], A. Rovida [(2)], A. Tertulliani[(1)]

[(1)] Istituto Nazionale di Geofisica e Vulcanologia, via di Vigna Murata 605, 00143 Rome, Italy

[(2)] Istituto Nazionale di Geofisica e Vulcanologia, via Alfonso Corti, 12 - 20133 Milan, Italy

Corresponding author: Laura Graziani laura.graziani@ingv.it

Abstract

The macroseismic source parameters of earthquakes occurring within a sequence are strongly influenced by cumulative damage effects. When we deal with historical seismic sequences, in addition to the cumulative intensities, other intrinsic uncertainties due to the scarcity and indeterminacy of sources come into play. These issues imply that the parameterizations of the single shocks within a historical seismic sequence are not univocal and that all the uncertainties that are addressed when assessing macroseismic intensity should be carefully considered in the parameter estimation. In the light of these considerations, we performed some tests on the 2016-2017 and 1703 seismic sequences, which occurred in the same area in Central Italy, to compute the macroseismic source parameters by means of two independent methods. Results show that the cumulative effects arising from multiple damaging shocks can cause biases in the intensity assessments, which affect the computed magnitude and epicentral locations. To reduce bias in macroseismic intensities due to cumulative damage, we illustrate a simple procedure, called Cumulative Intensity Subtraction (CIS), which consists in discarding the localities strongly damaged by the early earthquakes of a sequence from the intensity distributions used for computing the macroseismic source parameters of the subsequent shocks. The outcomes show that, for the 2016 seismic sequence, the CIS approach provides locations in agreement with the instrumental epicenters and with the causative faults. For the 1703 sequence the CIS approach along with explicit accounting for the indeterminacy in intensity assignments give a range of equally plausible solutions. The CIS represents an exploration of a simple strategy that stems from an attempt to give significance to macroseismic intensity in the presence of cumulative damage.

Introduction

Macroseismic intensity estimation is a methodology that allows historical and modern earthquakes to be studied in a comparative way. Intensity Data Points (IDP) are used to quantify, through

observations of macroseismic effects, the distribution and severity of earthquake damage and to obtain such quantitative parameters of the earthquakes as location, magnitude and even orientation of the seismogenic fault (Bakun and Wentworth, 1997; Gasperini et al., 1999, 2010; Pettenati and Sirovich, 2003; Vannucci et al., 2019). This is particularly important for assessing the seismotectonic features and/or the statistical properties of the seismicity in areas, such as most of Europe, where a large amount of written records about ancient earthquakes balances the availability of accurate and reliable instrumental locations and sizings, limited to the last few decades. Although empirically determined and possibly with different physical meaning, especially as far as the earthquake location is concerned, macroseismically determined source-parameters are commonly recognized to be reliable proxies when instrumental ones are lacking, and the similarity of macroseismically determined source-parameters with instrumentally determined ones for Italian earthquakes is widely documented in the literature (Cecic et al., 1996; Gasperini et al., 2010; Bakun et al., 2011; Gómez Capera et al; 2015; Vannucci et al., 2019). This assumption and the practice of merging instrumental source parametres with those assessed from intensity distributions into comprehensive long-term earthquake catalogs are widely accepted, in Europe (e.g Fäh et al., 2012; Grünthal and Wahlström, 2012; Rovida et al., 2020; Manchuel et al., 2019) and elsewhere (e.g Felzer and Cao, 2008; Beauval et al., 2013; Brax et al; 2019), especially in the framework of seismic hazard assessments. Indeed, this is a valuable method of comparing locations and magnitudes of contemporary and recent earthquakes with historical ones. When dealing with damaging seismic sequences, in which multiple earthquakes produce a superimposition of the effects, the intensity assessment and the following parametrization becomes critical. It is recognized that in seismic sequences the building stock undergoes a deterioration of the strength characteristics, with a progression of damage (Grimaz and Malisan, 2017; Penna et al., 2014), and, after multiple shocks, we observe a cumulative damage as a final result. The recurrence of damaging aftershocks makes the assessment of the macroseismic intensity related to each single

earthquake difficult, because of the complexity of estimating the vulnerability variations of the buildings and the progress of the grade of damage. Recent studies have stressed the issue of the assessment of macroseismic intensity during a seismic sequence (Graziani et al., 2017 and 2019; Rossi et al., 2019; Azzaro et al., 2019) suggesting that the contribution of the single earthquakes for the purpose of the intensity assessment is not recognizable.

Consequently, the assignment of some intensities based on cumulative damage is unavoidable, and might lead to an overestimation of such intensities, which then affect the macroseismically determined source parameters (Albini and Pantosti, 2004; Stucchi and Rovida, 2008; Graziani et al., 2019). A detailed field investigation of the evolution of damage during a modern sequence might result in the identification of the localities affected by cumulative effects. On the contrary, in the study of historical seismic sequences, the possibility of following the progression of the damage is hampered by the availability of the sources that describe in detail the evolution of the sequence, such as early reports and successive accounts. Very often reports provide information only on the cumulative effects, and do not allow to define the impact of individual shocks. It is a primary aim of the historical seismologist to define, as accurately as possible, the chronology of the shocks in order to give a description as faithful as possible of the sequence through the intensity distribution of the main earthquakes; unfortunately the assessment of the intensities is often based on suppositions rather than on robust inferences.

Therefore, the macroseismic source parameters, or simply macroseismic parameters, as defined in Cecic et al. (1996) and Musson and Cecic (2012), of earthquakes belonging to a sequence are influenced by cumulative damage effects, and when using such parameters, in particular for seismotectonic interpretations, one must be aware that they are affected by indeterminacies that should be taken into account.

The comparison with instrumental parameters can provide an estimate of the influence of the cumulative effects on the macroseismic parameters. In the case of historical seismic sequences the comparison with the instrumental data is not possible, and the chance of obtaining biased results is very high.

In this paper we present the parameterization of the 1703 seismic sequence in Central Italy using data from the recent reappraisal by Tertulliani et al. (2022), with the purpose of showing that the parameters of earthquakes within a historical sequence are not univocal and that all the issues that are addressed when assessing macroseismic intensity should be considered in the parameter estimation. In the light of these considerations, we made some tests to compute the macroseismic parameters of the 2016-2017 seismic sequence and compared them with instrumental data; the same tests are then applied to the 1703 sequence that is the historical sequence most similar to that of 2016-2017.

Macroseismic source parameters of the 2016-2017 seismic sequence

On August 24, 2016 a destructive seismic sequence began and hit a large area of Central Italy with several strong events within about five months. The main shocks occurred on August 24, 2016 (Mw 6.2), October 26, 2016 (Mw 6.1), October 30, 2016 (Mw 6.6) and January 18, 2017 (Mw 5.7, Mw 5.6) (Rovida et al., 2020; 2022).

During the sequence a progressive and noticeable worsening of damage to the building stock was observed (Fig. 1). The progression of damage to the buildings was monitored during many days of field campaigns by teams of experts in macroseismic surveys (Azzaro et al., 2016; Rossi et al., 2019, Galli et al. 2016; 2017).

The most comprehensive results of the field surveys of the main earthquakes of the sequence mentioned above, integrated with far-field data assessed through newspaper reports and interviews with local authorities, are presented in Rossi et al. (2019). The temporal spacing between the August

24 (Mw 6.2) and subsequent large shocks has allowed these authors to perform a well detailed macroseismic survey of the first earthquake, resulting in 221 IDPs with maximum intensity 10 EMS-98, before the damage scenario was upset by successive earthquakes. Unavoidably, the assessment of intensity after the October 26 (77 IDPs with maximum intensity 8 EMS-98) and 30 (379 IDPs with maximum intensity 11 EMS-98) events had to consider the cumulative damage, which made it impossible to determine the contribution of individual main-shocks to many cases of observed damage. Rossi et al. (2019) conclude that the observed clusters of very high values in their intensity distributions of the October 26 and 30 earthquakes can be due to the superposition of the effects of more than one earthquake. These authors also determine the macroseismic parameters of the main shocks by means of the Boxer code (Gasperini et al., 2010; hereinafter simply Boxer) with the same configuration used for the Italian Parametric Earthquake Catalogue CPTI15 (Rovida et al. 2020; 2022).

The resulting macroseismic epicenter for the August 24 earthquake (pink triangle in Fig. 2A) is close to the instrumental location (Margheriti et al., 2017), and its macroseismic magnitude is compatible with the instrumental moment magnitude determination (first row 'Boxer' column in Table 1). The macroseismic epicenter is also compatible with the maximum slip distribution proposed by Chiaraluce et al. (2017). On the contrary, the same calculation using the intensities after the October 30 shock provides a macroseismic location (pink triangle in Fig. 2B) nearly coinciding with the locations of the August 24 earthquake. Although a difference between the macroseismic and instrumental location is expected for events of this size, in this case the macroseismic solution is hardly compatible with the causative fault identified for the October 30 shock and the macroseismic epicenter does not match the area of maximum slip identified by (Chiaraluce et al., 2017). Moreover Bakun et al. (2011) identified a good agreement between extended sources and macroseismic epicenters of Italian earthquakes with $M \geq 6$. In addition, the distance between the instrumental and macroseismic epicenters of 18 km is

131 higher than the average (12.6 km) between the two solutions proposed by the Italian catalog CPTI15
132 (Rovida et al. 2020; 2022), which contains both types of estimates and assess macroseismic
133 parameters with the same method, for onshore earthquakes with M≥6. The macroseismic magnitude
134 of the October 30 earthquake is overestimated with respect to the instrumental value.
135 This result might be related to the location method of Boxer, which determines the epicenter as the
136 barycenter of the maximum intensities which, in this case, are clustered in the area already severely
137 affected by the August 24 earthquake as a consequence of cumulative damage.
138 To evaluate this hypothesis, we computed the macroseismic parameters of both earthquakes with an
139 independent method using the same datasets as Rossi et al. (2019). We selected the method of Bakun
140 and Wentworth (1997), hereinafter BW97, because, differently from Boxer, it calculates a
141 macroseismic magnitude over a grid of trial source locations by means of an Intensity Prediction
142 Equation (IPE) and determines the earthquake epicenter and the associated magnitude as the grid point
143 where the residuals are minimum. For the test, we chose a 200 x 200 km search grid, 2-km spaced,
144 centered on the instrumental epicenter and selected the most recent IPE proposed for Italy by Pasolini
145 et al. (2008), recalibrated with updated data from DBMI15 version 1.5 (Locati et al., 2016) by Lolli
146 et al. (2019).
147 The results obtained with BW97 (Table 1, Fig. 2) in terms of epicentral location for both the
148 earthquakes, are consistent with Boxer's results. Although BW97's epicenter of the October 30
149 earthquake, computed taking into account the whole spatial distribution of the intensities, seems less
150 influenced by the distribution of the maximum intensities - 13 km from the instrumental location
151 instead of 18 km of Boxer's - the effects caused by the cumulative damage is confirmed. However,
152 the confidence bounds of BW97's location (Fig. 2B), represented as the 0.02 rms contour according
153 to Bakun and Wentworth (1997), match the surface projection of the causative fault (Chiaraluce et al.,
154 2017), as happens with Italian events similar magnitudes analyzed in Bakun et al. (2011). The

uncertainty ellipse of the Boxer location, which we recomputed with the bootstrap resampling option provided by the code (see Gasperini et al., 2010) with 1000 resampled datasets, is much smaller than the fault projection, although their azimuths are similar.

In terms of magnitude BW97 results are not satisfying, because the macroseismic magnitude of the October 30 earthquake turns out to be underestimated by 0.4 m.u.. This is probably due to the selected IPE, which seems not appropriate for modeling the intensity attenuation of the October 30 earthquake, particularly the highest observed intensities and the fast decay of intensity within 50 km from the epicenter (Fig. 3). Indeed, the dataset used in the calibration of the IPE (Lolli et al., 2019) does not include the 2016 earthquakes, and other earthquakes with such a high magnitude and maximum intensities are a few in DBMI15. For this reason we also tested the only alternative up-to-date IPE for Italy in the literature (Gómez Capera et al., 2017), but it does not improve the fit of the data any better (Fig. 3), and its use did not improve BW97's magnitude.

As a further test, we calculated the parameters from the final cumulative intensity distribution (Fig. 4), i.e. considering the maximum intensity of all the localities at the end of the sequence (Rossi et al., 2019), regardless of the shock that caused them. Indeed, the cumulative scenario often represents the only available information for many sites, because it is independent of the timing of observation, and this is usually the case of historical earthquakes. The location resulting from the cumulative intensities with both algorithms is very close to the instrumental epicenter of the August 24 shock, i.e. where the intensities are most affected by the effects of both shocks, confirming the effect of cumulative damage, evidenced also for the October 30 shock. The macroseismic magnitude computed from the final cumulative intensity distribution is roughly the same - overestimated - as the macroseismic magnitude of the October 30 earthquake with Boxer, whereas BW97 provides a largely underestimated result, as already observed with the parametrization of the October 30 earthquake.

Testing the Cumulative Intensity Subtraction (CIS)

Macroseismic locations assessed with both Boxer and BW97 show that the presence of IDPs with intensity influenced by damage caused by the August 24 earthquake affect the determination of the macroseismic epicenter of the October 30 earthquake. We performed some tests in order to analyze and quantify the influence of the localities already heavily damaged on August 24 on the parameterization of the October 30 earthquake.

From a macroseismic point of view there is no simple rule for assessing how and how much the seismic performance of a building might be influenced by pre-existing damage. One can argue that after suffering moderate to heavy structural damage, starting at damage grade 3 according to the European Macroseismic Scale EMS-98 (Grünthal, 1998), the vulnerability of a building will certainly increase. In this case the building can behave very poorly, so that a relatively weak aftershock can cause a disproportionate amount of damage (Grünthal, 1998). In terms of macroseismic intensity we consider intensity 7 EMS-98 as the threshold above which a significant spreading of structural damage in the whole building stock can occur, and also cause a permanent weakening of buildings (Grimaz and Malisan, 2017). In fact, the low intensity degree, i.e. 6 EMS-98, does not foresee damage grade 3 in any vulnerability class, while in the high intensity degree, 8 EMS-98, all the vulnerability classes, except those including ERD buildings (with Earthquake Resistant Design), suffer structural damage. In addition, the adoption of this threshold is reasonable for Italy because about 80% of the building stock predates the 1980s (ISTAT, 2011) and the seismic building code for the whole Italian territory was enforced only since 2003 (Stucchi et al., 2011). If the 7 EMS-98 threshold has been exceeded earlier in the earthquake sequence, the damage produced by an aftershock is likely to be biased by a cumulative effect. Under this assumption we recalculated the macroseismic parameters of the October 30 earthquake excluding from the calculation IDPs with estimated intensity greater than 7 as a

consequence of the August 24 earthquake. We called this approach Cumulative Intensity Subtraction (CIS).

This exercise can be easily performed especially when the areas of maximum effects of each earthquake of the sequence are not coincident, but they share an overlapping area, where the cumulative effects are predominant and can be easily identified and subtracted.

Also in this case the tests were done with both Boxer and BW97 methods (Fig. 5 and Table 1), with the configurations described above. The locations obtained considering the CIS approach show that $\Delta epic$ is approximately reduced by half being 6.6 and 7.2 km for Boxer and BW97 respectively, mitigating the effects of cumulative intensities. Besides the consistency of the epicenters, especially BW97's and its confidence area, with the surface projection of the fault responsible for the October 30 earthquake is confirmed by the comparison with the areas of maximum slip calculated by Chiaraluce et al. (2017) as the centroid of the slip distribution is southeast of the instrumental epicenter by a few km (circa 4km). The macroseismic epicenters, calculated with CIS, are instead well suited to the maximum slip on the source.

Both CIS solutions are located to the east of the instrumental epicenter, at a similar latitude. This is a possible consequence of the asymmetry of the intensity distribution, with intensities values higher to the northeast of the epicenter than to the southwest, consistently with the lower attenuation of the ground motion towards the northeast (e.g. Luzi et al. 2017; Sgobba et al., 2021). In terms of magnitude, the subtraction from the calculation of many high IDPs, in particular those located at large distances from the calculated epicenters, produces estimates lower than those obtained with both methods from the cumulative intensity distribution, obviously characterized by higher and more widespread IDPs with high values. Our proposal represents an exploration of a simple strategy that addresses the issue of cumulative intensity distributions focussing on the definitions and meaning of intensity degrees.

What would happen in case of a non-instrumental earthquake? Macroseismic source parameters of the 1703 seismic sequence

The appraisal of the reliability of the macroseismic parameters of earthquakes belonging to a seismic sequence discussed above is even more challenging when dealing with historical events because of the difficulties in discriminating the contribution of the single shocks to the overall effects described in historical sources.

In order to evaluate the impact of such uncertainties on the location and magnitude of historical earthquakes, we repeated the tests performed on the 2016 earthquake sequence, with the intensity datasets related to a seismic sequence that hit the same area of Central Italy with a similar impact at the beginning of 1703. This sequence was one of the most catastrophic in the seismic history of Italy, and was characterized by two main strong events, on January 14 and February 2, 1703 resulting in a death toll of almost 10,000 victims (Tertulliani et al., 2022). Another earthquake, whose effects cannot be isolated from those of the first shock, occurred on January 16, 1703. The recent study of the 1703 seismic sequence by Tertulliani et al. (2022) reappraised the main earthquakes by considering the damage progression due to the multiple shocks. The sequence hit a territory almost equally divided between the Papal State and the Kingdom of Naples. After the earthquakes the two governments moved, for surveys and rescues, in different times and in different ways, producing an amount of sources and information often in contradiction to each other and superimposed. While the Papal's envoy (De Carolis, 1703) carried out a timely field survey in the territory of the Papal State struck by the January 14 earthquake, the Neapolitan officers reached the epicentral area only after the February 2 earthquake, consequently their damage descriptions refer to the cumulative effects of the two main events. For this reason the February 2 earthquake remains poorly described and unsolved with respect to what is outlined for the January 14 earthquake. Nevertheless, a letter found in the archive of Naples

(Archivio di Stato di Napoli, 1703a) provides information about many villages in the Kingdom of Naples that were already heavily damaged by the January 14 earthquake. Despite the generic nature, this account would confirm that part of the area of maximum damage due to the earthquake of 2 February was already devastated by the previous earthquake. Therefore the very high intensities, up to 10 EMS-98, in the entire area located northwest of L'Aquila may be due to the cumulative shaking of the two earthquakes (Fig. 7). This is a common feature with the 2016-2017 seismic sequence, as in both cases the second earthquake struck an area different from the epicentral area of the first earthquake but partially overlapping with it. As a main difference with respect to the 2016-2017 sequence, the most energetic shock was probably the first one, that occurred on January 14, 1703. This earthquake was thoroughly reconstructed, thanks to the documentation resulting from the timely intervention of the Papal State, in Tertulliani et al. (2022), who assessed 269 IDPs for this event with maximum intensity 11 EMS-98 at 8 localities (Fig. 6a), and 131 IDPs for the February 2 event with maximum intensity 11 EMS-98 at one locality (Fig. 7). In addition, there are 41 IDPs with intensity up to 10 EMS-98 for which the earthquake within the sequence that caused the described damage is not known, and they might equally belong to either the January 14 or February 2 intensity distribution (Uncertain Date Locality UDL; Fig. 6b).

These authors also highlighted that, particularly for historical seismic sequences, the intensity assessment is intrinsically affected by several kinds of uncertainties, due to the scarcity of written documentation, their haziness and cumulative damage. The fallout of these uncertainties is a loosely constrained distribution of IDPs, especially for the February 2 earthquake, with many localities assessed as widely (up to two degrees) uncertain intensity (hereinafter WUI, Widely Uncertain Intensity, represented with diamonds in Figures 7 and 10) due to vague accounts. For the February 2 earthquake, WUIs are mostly referred to all the villages, located in the area of the largest effects and

definitely damaged (Fig. 7), whose only information concerns the granting of tax exemption by the Naples Government without any direct damage description (Tertulliani et al., 2022; Fig. 8).

In order to verify the impact of all the mentioned uncertainties on the macroseismic parameters, we parameterized the new datasets by Tertulliani et al. (2022) of both earthquakes using both Boxer and BW97, with the same options and settings illustrated above for the 2016-2017 earthquakes. For the sake of simplicity, we treated uncertain intensity values and WUIs assuming once their maximum values, and subsequently their minimum values, not considering all possible intermediate combinations.

As mentioned above, the 14 January earthquake is well documented and the resulting intensity distribution is fairly well constrained, without any WUIs. We parameterized this earthquake at first without considering the 41 UDLs, and then adding them to the intensity dataset. The results of these two intensity distributions are very stable locations, independent from the inclusion or exclusion of the UDLs (Fig. 6). Indeed, all Boxer's solutions with "minimum" and "maximum" intensities and with or without UDLs, coincide, whereas BW97 epicenters are located only a few kilometers apart (less than 2.5 km), all within the respective uncertainty ranges.

In terms of magnitude the results obtained using Boxer and BW97 seem stable and independent from the contribution of the UDLs (Table 2). BW97 estimates are all lower than Boxer's and, taking into account the results of the 2016 events, they are probably underestimated.

As the seismic sequence advances, its data becomes more and more imprecise and all the uncertainties mentioned above become more significant. In fact, beside UDLs, the February 2 dataset includes 19 localities that are estimated with a widely uncertain intensity (WUI) due to vague accounts. The complexity of the February 2 dataset is further enhanced by the presence of cumulative effects. Localities marked with a square in Figure 7, according to the historical sources, were already damaged by the January 14 earthquake and their intensity is therefore the cumulative of the two earthquakes.

In addition, in our understanding, an area of overlapping effects, where localities already damaged by the January 14 earthquake may have experienced an aggravation of damage, could be reasonably identified (shaded area in Fig. 7).

As the 2016-2017 seismic sequence, also the two main earthquakes of 1703 show a partial overlap of the areas of greatest effects and therefore are well suited for the application of the CIS approach. However, in this case the uncertainties in the February 2 dataset prevent the definition of a unique outline of the intensity distribution, so we assumed seven different plausible scenarios to compute the macroseismic parameters of the February 2 earthquake:

- scenario #1a: without UDLs;
- scenario #1b: with UDLs;
- scenario #2a: without UDLs applying the CIS method - excluding from the intensity distribution IDPs already damaged (I>7) by the previous shock (marked with a square in Figure 7);
- scenario #2b: with UDLs applying the CIS method - excluding from the intensity distribution IDPs already damaged (I>7) by the previous shock;
- scenario #3a: same as scenario#2a applying the CIS method - excluding from the intensity distribution also those localities that we assume may have been affected by the cumulative effects - (IDPs to the NW of L'Aquila in the shaded area in Figure 7);
- scenario #3b: same as scenario#2b applying the CIS method - excluding from the intensity distribution also those localities that we assume may have been affected by the cumulative effects - (IDPs to the NW of L'Aquila in the shaded area in fig. 7) (Fig. 9e, 9f);
- scenario #4: cumulative intensity distribution resulting from the two shocks (Fig. 10).

For all the listed scenarios we calculated macroseismic parameters by applying both Boxer and BW97 methods, considering separately the minimum and the maximum values for uncertain intensities and WUIs, obtaining four different solutions for each scenario.

If we look at the different locations of the macroseismic epicenters, from scenario 1 to scenario 3 (Fig. 9a to 9f), we can point out that:

- Scenarios 1a and 1b (Fig. 9a and 9b) display a very similar location of Boxer and BW97 solutions, with both minimum and maximum intensity values. The macroseismic epicenters are all clustered to the NW of L'Aquila within a range of a few (<10) kilometers.
- Scenarios 2a and 2b (Fig. 9c and 9d), applying the CIS method, show the epicenters moving to the SE toward L'Aquila, mitigating the bias of cumulative effects due to the localities already damaged during the January 14 earthquake (marked with the square in Figure 7).
- Scenarios 3a and 3b (Fig. 9e and 9f) show a further shift of the epicenters towards the SE, going beyond L'Aquila.
- In scenario 4 (cumulative intensity distribution, Fig. 10) the macroseismic epicenter of the February 2 shock coincides with the January 14 one or is very close to it. The cumulative scenario confirms the same behavior already seen with the 2016 sequence, regardless of the order of occurrence of the shocks and their magnitude.

All the epicenters obtained for the February 2 shocks, considering the different scenarios, are arranged along a 30 km NW-SE belt around L'Aquila (Fig. 11). In that area several fault traces have been identified in the literature, especially in the aftermath of the 6 April 2009 Mw 6.3 earthquake (e.g. Moro et al., 2002; 2013; Galli et al., 2010, 2011; Cinti et al., 2011; Faure Walker et al., 2021).

In terms of magnitude (Table 3), BW97 estimates from all the scenarios of the February 2 earthquake are slightly lower than Boxer's. For each scenario large differences between the minimum and

maximum estimate results from both methods, because of the presence of many WUI, whereas differences are limited comparing all the minimum and maximum values resulting from the different scenarios. As far as the cumulative intensity distribution is concerned, Boxer's magnitudes are very stable, regardless of the method and all the considered uncertainties (M 6.98-6.97 for Boxer, and 6.68-6.87 for BW97).

Conclusions

Rossi et al. (2019), in their macroseismic study of the 2016-2017 seismic sequence, highlighted the influence of the accumulation of damage on the macroseismic parameters of the second strong shock of October 30. The progressive occurrence of strong earthquakes entailed a saturation of damage levels so that the resulting cumulative scenario does not adequately reflect the effects of the individual shocks. Separating the influence of successive earthquakes on the vulnerability and damage of the buildings, which reflects on both the intensity assessment and the earthquake source parameters derived from it, is hardly possible even in the case of modern sequences whose effects can be monitored in real-time. The case of historical earthquake sequences is worsened by the difficulty of referring written accounts to one or the other shocks.

The aim of this work is to verify the influence of such cumulative damage effects on the determination of the macroseismic parameters of historical earthquakes close in space and time, through the analysis of the strongest earthquakes within the January-February 1703 seismic sequence Central Italy, which is considered "almost twin" of the 2016-2017 one, and was recently re-evaluated by Tertulliani et al. (2022).

We propose a method, called CIS (Cumulative Intensity Subtraction), that discards from the dataset used for computing macroseismic parameters of an aftershock the localities which suffered moderate to heavy structural damage to the whole building stock, corresponding to intensity 7 EMS-98 and

366 above, during the first earthquake. Above this threshold we suppose a permanent weakening of
367 buildings, so that the damage produced by an aftershock might be considered biased by a cumulative
368 effect.
369 We tested the CIS method with the intensity distributions of the 2016-2017 seismic sequence from
370 Rossi et al. (2019), comparing the locations and magnitudes obtained with two independent
371 algorithms, Boxer (Gasperini et al., 2010) and BW97 (Bakun and Wentworth, 1997), from the dataset
372 recently published by Tertulliani et al. (2022).
373 The results of the 2016-2017 sequence suggest that with the CIS approach it is possible to obtain a
374 macroseismic location more representative of the instrumental epicenter,the causative faults and the
375 maximun slip distribution (Fig. 5) than with the cumulative intensity distribution (Fig. 4). Indeed, the
376 inclusion of cumulative intensities in the calculation causes the macroseismic epicenter to shift
377 towards the epicentral area of the most damaging event. This is confirmed either by the use of
378 cumulative intensity of an aftershock or of the whole sequence. These results encouraged us to apply
379 this approach also to the 1703 sequence. In this case, partial knowledge of the effects of the sequence
380 results in a number of possible scenarios for the second earthquake that give rise to a range of different,
381 equally plausible, solutions (Fig. 11). For instance, the first four scenarios (1a, 1b, 2a, 2b) show very
382 similar epicentral locations, all compatible with the Upper Aterno Valley Fault System (UAVFS), NW
383 of L'Aquila (Fig. 10) (among the others Blumetti 1995; Moro et al. 2002), whereas scenarios 3a and
384 3b provide epicentral locations close to the Paganica fault, to the southeast of L'Aquila (Fig. 10)
385 (among the others Galli et al., 2011; Moro et al., 2013). In addition, considering the variability of the
386 magnitudes obtained for the different scenarios of the February 2 earthquake, between M6.5 and M7.1,
387 we may not exclude the contemporary activation of both segments.
388 At the same time, the uncertainties in the historical information related to the 1703 sequence and in
389 the assessment of its macroseismic intensities, affect more significantly the estimated magnitude

rather than the location, whereas the two independent codes we used show results in good agreement between them, provided that robust IPEs are developed.

The proposed CIS approach should be further tested with other historical sequences, although the number of modern sequences against which to test the results is (luckily) very limited. However, the different results allow us to conclude that, for earthquakes within historical seismic sequence, whose basic data have substantial uncertainty, there may not be preferred macroseismic solutions but rather a set of possible hypotheses. Therefore, when using macroseismic parameters of historical earthquakes for seismotectonic interpretations we must not overlook the role and the weight of epistemic indeterminacy.

Data and resources

Catalogo Parametrico dei Terremoti Italiani (CPTI15) catalog (Rovida et al., 2022) and Database Macrosismico Italiano (DBMI15) (Locati et al., 2016) data are collected at https://emidius.mi.ingv.it/CPTI15-DBMI15/. Bollettino Sismico Italiano (BSI) data are from Margheriti et al., (2017) at https://doi.org/10.13127/BSI/201602

Acknowledgements

The Authors wish to thank the Associate Editor and the anonymous reviewer who contributed to improve the manuscript with precious comments and suggestions.

Declaration of Competing Interests

The authors acknowledge there are no conflicts of interest recorded.

References

Albini, P., D. Pantosti (2004). The 20 and 27 April 1894 (Locris, Central Greece) Earthquake Sources through Coeval Records on Macroseismic Effects, *Bull. Seism. Soc. Am.* **94**(4):1305-1326 http://dx.doi.org/10.1785/012003174

Archivio di Stato di Napoli (1703a). Consiglio Collaterale, Notamenti, 107, cc. 97v-98r, manuscript.

Archivio di Stato di Napoli (1703b). Regia Camera della Sommaria, Notamentorum, fascio 144, manuscript.

Azzaro, R., M. S. Barbano, A. Tertulliani , C. Pirrotta (2019). A reappraisal of the 1968 Valle del Belìce seismic sequence (Western Sicily): a case study of intensity assessment with cumulated damage effects. *Ann. Geophys.* **63**, 1, SE105. https://doi.org/10.4401/ag-8308.

Azzaro, R., A. Tertulliani, F. Bernardini, R. Camassi, S. Del Mese, E. Ercolani, L. Graziani, M. Locati, A. Maramai, V. Pessina, A. Rossi, A. Rovida, P. Albini, L. Arcoraci, M. Berardi, C. Bignami, B. Brizuela, C. Castellano, V. Castelli, S. D'amico, V. D'amico, A. Fodarella, I. Leschiutta, A. Piscini, M. Sbarra (2016). The Amatrice 2016 earthquake: macro-seismic survey in the damage area and preliminary EMS intensity assessment. *Ann. Geophys*. **59**, FAST TRACK 5, https ://doi.org/10.4401/ag-7203.

Bakun, W.H., A. Gómez Capera, M. Stucchi (2011). Epistemic Uncertainty in the Location and Magnitude of Earthquakes in Italy from Macroseismic Data. *Bull. Seismol. Soc. Am.* **101**, 2712–2725. https://doi.org/10.1785/0120110118

Bakun, W.H., C.M. Wentworth (1997). Estimating earthquake location and magnitude from seismic intensity data. *Bull. Seismol. Soc. Am*. **87**, 1502–1521.

Beauval C., H. Yepes, P. Palacios, M. Segovia, A. Alvarado, Y. Font, J. Aguilar, L. Troncoso, S. Vaca (2013). An Earthquake Catalog for Seismic Hazard Assessment in Ecuador. *Bull. Seism. Soc. Am.* **103**, 773–786. doi: https://doi.org/10.1785/0120120270

Blumetti, A.M. (1995). Neotectonic investigation and evidence of paleoseismicity in the epicentral area of the January–February 1703, Central Italy, earthquakes. In: Serva, L., Slemmons, B. (Eds.), *Perspectives in Paleoseismology*. Special Publication-Association of Engineering Geologists **6**, 83–100.

Cecic, I., Musson, R.M.W., Stucchi, M. (1996). Do seismologists agree upon epicentre determination from macroseismic data? A survey of ESC Working Group "Macroseismology". *Ann. Geoph.* **39**, 1013-1027. https://doi.org/10.4401/ag-4031

Chiaraluce, L., R. Di Stefano, E. Tinti, L. Scognamiglio, M. Michele, E. Casarotti, S. Marzorati (2017). The 2016 Central Italy Seismic Sequence: a first look at the Mainshocks, aftershocks, and source models. *Seismol. Res. Lett.* **88**, 757–771. https://doi.org/10.1785/0220160221

Cinti, F.R., D. Pantosti, P.M. DeMartini., S. Pucci, R. Civico, S. Pierdominici, L. Cucci (2011). Evidence for surface faulting events along the Paganica Fault prior to the April 6, 2009 L'Aquila earthquake (Central Italy). *J. Geophys. Res.* **116**. http://dx.doi.org/10.1029/2010JB007988.

De Carolis, P. (1703). Relazione generale delle ruine, e mortalità cagionate dalle scosse del Terremoto de' 14 Gennaro, e 2 Febbraro 1703 in Norcia, e Cascia, e loro contadi, compresi li Castelli delle Rocchette, e Ponte, Giurisdizione di Spoleto. Roma. In Italian.

Fäh, D., D. Giardini, P. Kästli, N. Deichmann, M. Gisler, G. Schwarz-Zanetti, S. Alvarez-Rubio, S. Sellami, B. Edwards, B. Allmann, F. Bethmann, J. Wössner, G. Gassner-Stamm, S. Fritsche, D. Eberhard (2011). ECOS-09 Earthquake Catalogue of Switzerland Release 2011 report and database, Swiss Seismological Service ETH Zurich, Rep. SED/RISK/R/001/20110417.

Faure Walker, J., P. Boncio, B. G. Pace, L. Roberts, O. Benedetti Scotti, F. Visini, L. Peruzza (2021). Fault2SHA Central Apennines database and structuring active fault data for seismic hazard assessment. *Sci Data*, **8**, 87. https://doi.org/10.1038/s41597-021-00868-0.

Felzer K.R., T. Cao (2008). WGCEP Historical California earthquake catalog, Appendix H in The Uniform California Earthquake Rupture Forecast, version 2 (UCERF 2). U.S. Geological Survey, Open-File Report 2007-1437H and California Geological Survey Special Report 203H, 127 pp. https://pubs.usgs.gov/of/2007/1437/h/

476 Galli, P., B. Giaccio, P. Messina (2010). The 2009 central Italy earthquake seen through 0.5 Myr-long
477 tectonic history of the L'Aquila faults system. *Quaternary Science Reviews* **29**, 3768–3789.
478 http://dx.doi.org/10.1016/j.quascirev.2010.08.018.
479
480 Galli, P. , B. Giaccio, P. Messina, E. Peronace and G. M. Zuppi (2011). Palaeoseismology of the
481 L'Aquila faults (central Italy, 2009, Mw 6.3earthquake): implications for active fault linkage,
482 *Geophys. J. Int.*, **187**, 1119–1134 doi: 10.1111/j.1365-246X.2011.05233.x.

483 Galli P., Peronace E., Bramerini F., Castenetto S., Naso G., Cassone F., Pallone F. (2016). The MCS
484 intensity distribution of the devastating 24 August 2016 earthquake in central Italy (Mw 6.2). *Ann.*
485 *Geophys.*, **59**, Fast Track 5, 13 pp. https://doi.org/10.4401/ag-7287

486 Galli, P., Castenetto, S., Peronace, E., (2017). The macroseismic intensity distribution of the 30
487 October 2016 earthquake in Central Italy (Mw 6.6): Seismotectonic implications. *Tectonics* **36**, 1–13.
488 https://doi.org/10.1002/2017tc00458.

489 Gasperini, P., F. Bernardini, G. Valensise, E. Boschi (1999). Defining seismogenic sources from
490 historical earthquake felt reports. *Bull. Seismol. Soc. Am.* **89**, 94–110.
491
492 Gasperini, P., G. Vannucci, D. Tripone and E. Boschi (2010). The location and sizing of historical
493 earthquakes using the attenuation of macroseismic intensity with distance. *Bull. Seism. Soc. Am.*, **100**,
494 2035–2066.

Gómez Capera, A.A., A. Rovida, P. Gasperini, M. Stucchi, D. Viganò (2015). The Determination of Earthquake Location and Magnitude from Macroseismic Data in Europe. *Bull. Earthq. Eng*. **13**, 1249-80. https://doi.org/10.1007/s10518-014-9672-3.

Gómez Capera, A.A., M. Santulin, M. D'Amico, V. D'Amico, M. Locati, L. Luzi, M. Massa, C. Meletti (2017). Italian Macroseismic Intensity Attenuation Model as a function of Mw and distance. Proceed. 36° GNGTS Conference, Trieste, http://www3.ogs.trieste.it/gngts/files/2017/S21/Riassunti/GomezCapera2.pdf.

Graziani, L., A. Tertulliani, A. Maramai, A. Rossi and L. Arcoraci (2017). The 1984 Abruzzo- Latium seismic sequence: reappraisal of the existing macroseismic datasets according to the EMS98. *J. Seismol.,* **21**, 1-9, doi:10.1007/s10950-017-9663-3.

Graziani, L., S. Del Mese, A. Tertulliani, L. Arcoraci, A. Maramai and A. Rossi (2019). Macroseismic assessment (EMS-98) of damage progression during the 2016-17 seismic sequence in Central Italy, *Bull. Earthq. Eng* **17**, 5535–5558, https://doi.org/10.1007/s10518-019-00645-w.

Grimaz, S. and P. Malisan (2017). How could cumulative damage affect the macroseismic assessment? *Bull. Earthq. Eng.* **15**, 2465–2481, DOI 10.1007/s10518-016-0016-3.

Grünthal, G. (Ed.). (1998). European Macroseismic Scale 1998 (EMS-98). European Seismological Commission, sub commission on Engineering Seismology, Working Group Macroseismic Scales. Conseil de l'Europe, Cahiers du Centre Européen de Géodynamique et de Séismologie 15. Luxembourg, pp. 99, http://www.ecgs.lu/cahiers-bleus/.

Grünthal, G., R. Wahlström (2012). The European-Mediterranean Earthquake Catalogue (EMEC) for the last millennium. *J. Seismol.* **16**, 535-570, https://doi.org/10.1007/s10950-012-9302-y.

ISTAT (2011) 15° censimento generale della popolazione e delle abitazioni. Istituto Nazionale di Statistica, Roma. (In Italian).

Locati, M., R. Camassi, A. Rovida, E. Ercolani, F. Bernardini, V. Castelli, C.H. Caracciolo, A. Tertulliani, A. Rossi, R. Azzaro, S. D'Amico, S. Conte and E. Rocchetti (2016). DBMI15, the 2015 version of the Italian Macroseismic Database. Istituto Nazionale di Geofisica e Vulcanologia. http://doi.org/10.6092/INGV.IT-DBMI15.

Lolli, B., C. Pasolini, P. Gasperini and G. Vannucci (2019). Prodotto 4.8: Ricalibrazione dell'equazione di previsione di Pasolini et al. (2008). In: Meletti C. and W. Marzocchi (eds.): Il modello di pericolosità sismica MPS19. Rapporto finale, Centro Pericolosità Sismica, Istituto Nazionale di Geofisica e Vulcanologia, maggio 2019, Roma, 168 pp. + 2 App. In Italian.

Luzi, L., F. Pacor, R. Puglia, G. Lanzano, C. Felicetta, M. D'Amico, A. Michelini, L. Faenza, V. Lauciani, I. Iervolino, G. Baltzopoulos, E. Chioccarelli (2017). The Central Italy Seismic Sequence

between August and December 2016: Analysis of Strong Motion Observations. *Seismol. Res. Lett.*, **88**, 1219–1231. doi: https://doi.org/10.1785/0220170037

Margheriti, L., A. Nardi, F. M. Mele, A. Marchetti (2017). Bollettino Sismico Italiano (BSI), II quadrimestre 2016 (Version 1). Istituto Nazionale di Geofisica e Vulcanologia (INGV). https://doi.org/10.13127/BSI/201602

Manchuel, K., P. Traversa, D. Baumont, M. Cara, E. Nayman, C. Durouchoux (2018). The French seismic CATalogue (FCAT-17). *Bull. Earthq. Eng.* **16**, 2227-2251, https://doi.org/10.1007/s10518-017-0236-1.

Moro, M., V. Bosi, F. Galadini, P. Galli, B. Giaccio, P. Messina, A. Sposato (2002). Analisi paleosismologiche lungo la faglia del M. Marine (alta valle dell'Aterno): risultati preliminari. *Il Quaternario*, **15**, 267-278. in Italian

Moro, M., S. Gori, E. Falcucci, M. Saroli, F. Galadini, S. Salvi (2013). Historical earthquakes and variable kinematic behaviour of the 2009 L'Aquila seismic event (central Italy) causative fault, revealed by paleoseismological investigations, *Tectonoph.*, **583**, 131–144, http://dx.doi.org/10.1016/j.tecto.2012.10.036.

Musson, R.M.W, I. Cecić (2012). Intensity and Intensity Scales. In: P. Bormann (Ed.), New Manual of Seismological Observatory Practice 2 (NMSOP-2), Deutsches GeoForschungsZentrum GFZ, Potsdam, 1–41, https://doi.org/10.2312/GFZ.NMSOP-2_ch12

Pasolini, C., D. Albarello, P. Gasperini, V. D'Amico, B. Lolli (2008). The attenuation of seismic intensity in Italy part II: modeling and validation. *Bull. Seismol. Soc. Am*. **98**, 692–708. https://doi.org/10.1785/0120070021.

Penna, A., P. Morandi, M. Rota, C.F. Manzini, F. da Porto, G. Magenes (2014). Performance of masonry buildings during the Emilia 2012 earthquake. *Bull. Earthq. Eng.* **12**, 2255–2273.

Pettenati, F., L. Sirovich (2003). Tests of source-parameter inversion of the U.S. Geological Survey intensities of the Whittier Narrows, 1987 earthquake. *Bull. Seismol. Soc. Am*. **93**, 47–60.

Rossi, A., A. Tertulliani, R. Azzaro, L. Graziani, A. Rovida, A. Maramai, V. Pessina, S. Hailemikael, G. Buffarini, F. Bernardini, R. Camassi, S. Del Mese, E. Ercolani, A. Fodarella, M. Locati, G. Martini, A. Paciello, S. Paolini, L. Arcoraci, C. Castellano, V. Verrubbi and M. Stucchi (2019). The 2016-2017 earthquake sequence in Central Italy: macroseismic survey and damage scenario through the EMS-98 intensity assessment. *Bull. Earth. Eng.*, **17**, 2407–2431, https://doi.org/10.1007/s10518-019-00556-w.

Rovida, A., M. Locati, R. Camassi, B. Lolli, P. Gasperini (2020). The Italian earthquake catalogue CPTI15. *Bull. Earth. Eng.*, **18**, 2953-2984. https://doi.org/10.1007/s10518-020-00818-y.

Rovida, A., M. Locati, R. Camassi, B. Lolli, P. Gasperini, A. Antonucci (2022). Italian Parametric Earthquake Catalogue (CPTI15), version 4.0. Istituto Nazionale di Geofisica e Vulcanologia (INGV). https://doi.org/10.13127/CPTI/CPTI15.4.

579 Sgobba, S., G. Lanzano, F. Pacor (2021). Empirical nonergodic shaking scenarios based on spatial
580 correlation models: An application to central Italy. *Earthquake Eng. Struct. Dyn.*, **50**, 60-80.
581 https://doi.org/10.1002/eqe.3362.

582 Stucchi, M. and A. Rovida (2008). Investigating Historical Earthquake Sequences, MERCEA'08
583 Seismic Engineering International Conference, Messina e Reggio Calabria 8-11 luglio 2008.
584

585 Stucchi M., C. Meletti, V. Montald, H. Crowley, G.M. Calvi, and E. Boschi (2011). Seismic Hazard
586 Assessment (2003–2009) for the Italian Building Code, *Bull. Seismol. Soc. Am.*, 101, 4, 1885–1911,
587 doi: 10.1785/0120100130
588

589 Tinti, E., L. Scognamiglio, A. Michelini and M. Cocco (2016). Slip heterogeneity and directivity of
590 the ML 6.0, 2016, Amatrice earthquake estimated with rapid finite-fault inversion. *Geophys. Res. Lett.*,
591 **43,** 10,745-10,752, https://doi.org/10.1002/2016GL071263.

592 Tertulliani, A., L. Graziani, M. Locati (2022). Nuovo studio della sequenza sismica del 1703 in Italia
593 centrale, *Quad. Geofis.*, 178, 1-578, https://doi.org/10.13127/qdg/178 . (In Italian)
594

595 Vannucci, G., P. Gasperini, B. Lolli, L. Gulia (2019). Fast characterization of sources of recent Italian
596 earthquakes from macroseismic intensities, *Tectonophysics* **750**, 70–92,
597 https://doi.org/10.1016/j.tecto.2018.11.002
598
599

Laura Graziani – Istituto Nazionale di Geofisica e Vulcanologia, Rome, Italy laura.graziani@ingv.it
ORCID: 0000-0003-4088-7841

Andrea Rovida – Istituto Nazionale di Geofisica e Vulcanologia, Milan, Italy andrea.rovida@ingv.it
ORCID: 0000-0001-6147-9981

Andrea Tertulliani – Istituto Nazionale di Geofisica e Vulcanologia, Rome, Italy andrea.tertulliani@ingv.it ORCID: 0000-0002-3746-0858

610 List of figures' captions

611

Figure 1 Example of cumulative damage during the 2016-2017 Central Italy seismic sequence to the same house after the August 24 (left) and after the October 30 shocks (right) (adapted with the permission from Graziani et al., 2019).

Figure 2 - Macroseismic epicenters (BW97=blue and BOXER=pink) compared with the instrumental determination (white stars) for the August 24 earthquake (left) and the October 30 earthquake (right). The distance (Δepic) between the macroseismic epicenters and the instrumental one is about 4.5 km for the August 24 earthquake and varies from 18 (BOXER) to 13 km (BW97) for the October 30 earthquake. The blue line is the confidence bound of the BW97 location, and the pink line is the uncertainty ellipse of the Boxer location. Intensity data from Rossi et al. (2019). The asterisks represent the centroids of the maximum slip distribution of the August 24 (southernmost) and October 30 (northernmost) earthquakes from Chiaraluce et al. (2007). The sources of the August 24 (from Tinti et al., 2016) and October 30 (from Chiaraluce et al., 2017) earthquakes are shown. The location of the two October 30 macroseismic epicenters (right) is driven by the highest intensities due to cumulative effects towards the location of the August 24 earthquake (small white star).

Figure 3 - Intensity attenuation of the October 30, 2016 earthquake data (grey dots) compared with the IPEs of Lolli et al. (2019) and Gómez Capera et al. (2017).

Figure 4 - Macroseismic epicenters (BW97=blue and BOXER=pink) calculated from the final cumulative intensity distribution. As in the case of the October 30 earthquake (see Fig. 3), the epicenters are dragged by cumulative intensities towards the epicenter of August 24, 2016 (small white star). The blue line is the confidence bound of the BW97 location, and the pink line is the uncertainty ellipse of the Boxer location. The sources of the August 24, 2016 (from Tinti et al., 2016) and October 30, 2016 (from Chiaraluce et al., 2017) earthquakes are shown. The asterisks represent the centroids of the maximum slip distribution of the August 24 (southernmost) and October 30 (northernmost) earthquakes from Chiaraluce et al. (2007).

Figure 5 - October 30 macroseismic epicenters calculated with the CIS method: IDPs with I>7 resulting from the August 24, 2016 shock (empty circles) are discarded from the computations. The epicenters (BW97=blu and BOXER=pink) are in good agreement with the instrumental one (big white star) and with the surface projection of the causative fault according to Chiaraluce et al. (2017). The blue line is the confidence bound of the BW97 location, and the pink line is the uncertainty ellipse of the Boxer location. The source of the August 24, 2016 (from Tinti et al., 2016) is also shown. The asterisks represent the centroids of the maximum slip distribution of the August 24 (southernmost) and October 30 (northernmost) earthquakes from Chiaraluce et al. (2007).

Figure 6. Intensity distribution and macroseismic epicentres derived from the minimum and maxi intensities of the January 14 earthquake dataset without (a) and with the UDLs (b). UDLs are indi with black empty squares. The dashed line is the boundary between the Papal State (to the nortl west) and the Kingdom of Naples (to the southeast).

Figure 7 Map of the intensities of February 2, 1703 (Tertulliani et al., 2022). The orange line represents the state border between the Papal State and the Naples Kingdom. The localities marked with a square were already damaged by the January 14th earthquake. The shaded area is the territory reasonably influenced by cumulative effects.

Figure 8 a) Excerpt from one of the lists of locations benefiting from tax exemption found in the Naples State Archive (Archivio di Stato di Napoli, 1703b). The frame indicates the zoom in Figure 8b. b) Magnification of the text in the box of Figure 8a, text translation "*L'Aquila for 8 or 10 years exempted from payments to the Court and to creditors, Amatrice for 4 or 5 years exepted as above, Acumoli for 2 or 3 years exempted as above*".

Figure 9 Six different scenarios for the parametrization of the February 2 earthquake: a) witho UDLs; b) with UDLs; c) applying the CIS method without UDLs; d) applying the CIS method, wi UDLs; e) applying the CIS method without UDLs and localities assumed as affected by tl cumulative effects; f) applying the CIS method with UDLs and without localities assumed affected by the cumulative effects. The dashed line is the boundary between the Papal State (to the north and west) and the Kingdom of Naples (to the southeast).

Figure 10 - Map of the cumulative IDPs for the whole 1703 sequence. For each locality the maximum intensity recorded is considered, regardless of the causative earthquake. The dashed line is the boundary between the Papal State (to the north and west) and the Kingdom of Naples (to the southeast). The blue line is the confidence bound of the BW97 location, and the pink line is the uncertainty ellipse of the Boxer location.

Figure 11 - Synthesis of the epicentral locations of the February 2 earthquake obtained from intensity distributions corresponding to Scenarios #1 to #3. For each scenario the solutions considering separately the minimum and the maximum values for uncertain intensities and WUIs are shown with the samne symbol, whereas some of the obtained locations are visible because they are coincident with others (see figure 9). Fault traces modified after Faure Walker et al. (2021); UAVFS =Upper Aterno Valley Fault System.

612

Tables

Table 1- Synthesis of the macroseismic parameters obtained with Boxer and BW97 from the intensity data (from Rossi et al., 2019) of the August 24, and October 30, 2016, from the CIS approach and from the cumulative intensities. BW97 Instrumental location (from Margheriti et al., 2017) and magnitude (Rovida et al., 2022) are also shown for comparison. Δepic and Δslip are the distances between instrumental and the macroseismic epicenter and, respectively, the macroseismic epicenter and the maximum slip centroid according to Chiaraluce et al. (2017). Mdp stands for the number of Macroseismic data points, LatUnc and LonUnc stand for latitude and longitude uncertainty expressed in km.

Earthquake			Boxer							BW97						Instrumental				
	Mdp	Imax	Lat (°N)	LatUnc (km)	Lon (°E)	LonUnc (km)	Mw	Δepic (km)	Δslip (km)	Lat (°N)	Lon (°E)	Mw	Mw Min/Max	Δepic (km)	Δslip (km)	Lat (°N)	LatUnc (km)	Lon (°E)	LonUnc (km)	Mw
24 August	221	10	42.683	2.692	13.278	0.599	6.45 ± 0.07	4.4	3.2	42.687	13.287	5.63	5.62/5.65	4.7	3.3	42.698	0.154	13.233	0.132	6.18±0.07
30 October	377	11	42.717	3.129	13.259	1.126	6.99 ± 0.05	18.0	16.3	42.759	13.233	6.18	6.17/6.20	13.0	11.1	42.830	0.187	13.109	0.111	6.61±0.07
30 Oct.CIS	322	9	42.813	6.626	16.18	2.162	6.20 ± 0.06	6.6	5.1	42.831	13.197	6.08	6.07/6.10	7.2	3.4	--	--	--		--
Cumulative	475	11	42.708	2.837	13.262	0.920	6.97 ± 0.05	--	--	42.759	13.215	6.09	6.09/6.11	--	--	--	--	--		--

Table 2 - Synthesis of the results of the magnitude computation for January 14 1703 scenarios.

Event scenario	**Mw Boxer(min-max)**	**Mw BW97(min-max)**
January 14	6.91-6.91	6.56-6.64
January 14 + UDLs	6.91-6.93	6.55-6.66

Table 3 - Synthesis of the results of the magnitude computations for all the February 2 1703 scenarios and the cumulative one.

Event scenario	**Mw Boxer(min-max)**	**Mw BW97(min-max)**
February 2 scenario #1a	6.61-6.99	6.53-6.75
February 2 scenario #1b	6.62-7.06	6.50-6.74
February 2 scenario #2a	6.58-6.99	6.37-6.63
February 2 scenario #2b	6.59-7.07	6.38-6.63
February 2 scenario #3a	6.52-7.03	6.22-6.47
February 2 scenario #3b	6.59-7.08	6.27-6.52
Cumulative scenario #4	6.98-6.97	6.68-6.87

Figure

Click here to access/download;Figure;Fig1A.jpg

Figure

Click here to access/download;Figure;Fig1B.jpg

Figure

Click here to access/download;Figure;Fig2A-B.jpg

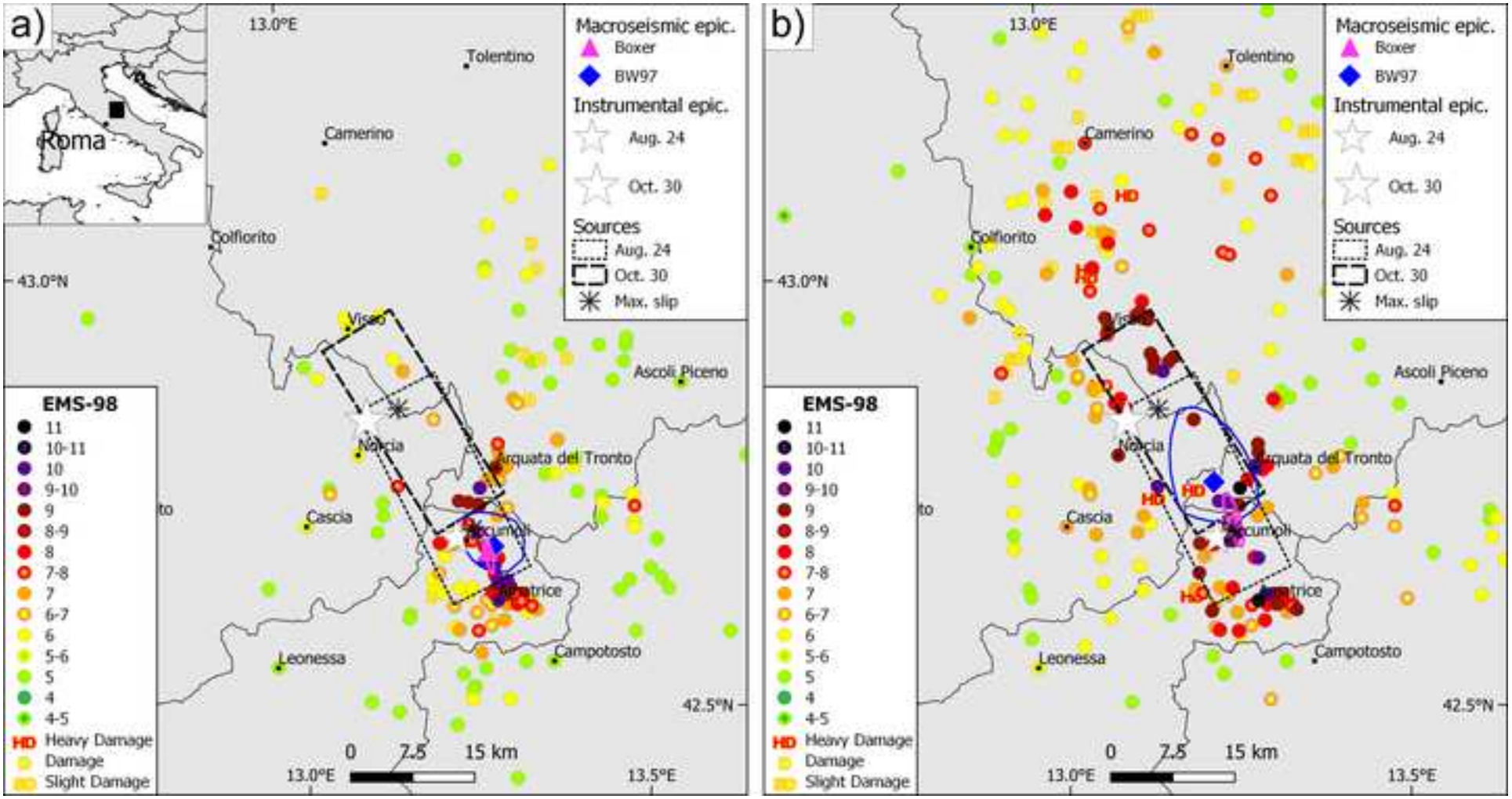

Figure

Click here to access/download;Figure;Fig3.jpg

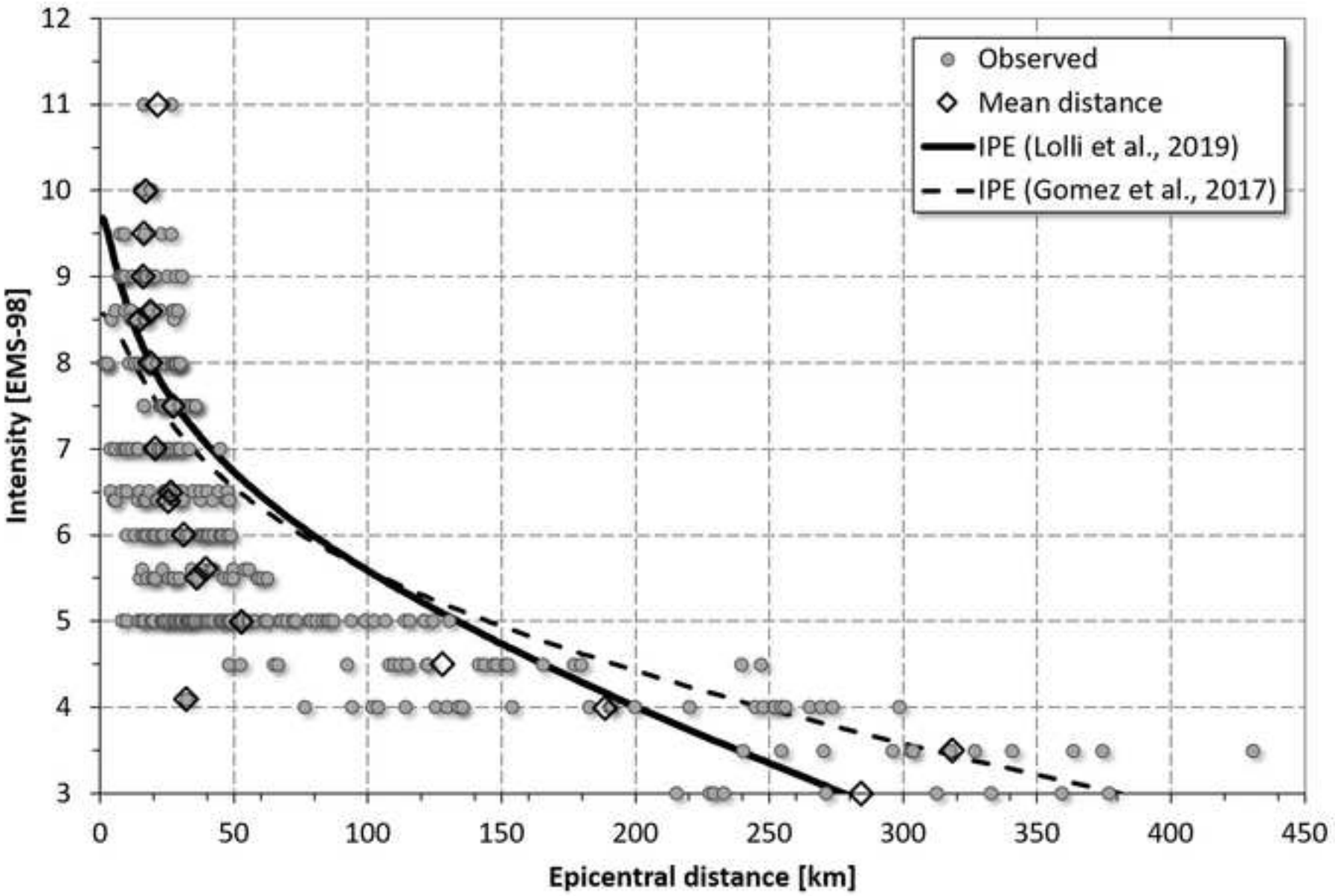

Figure

Click here to access/download;Figure;Fig4.jpg

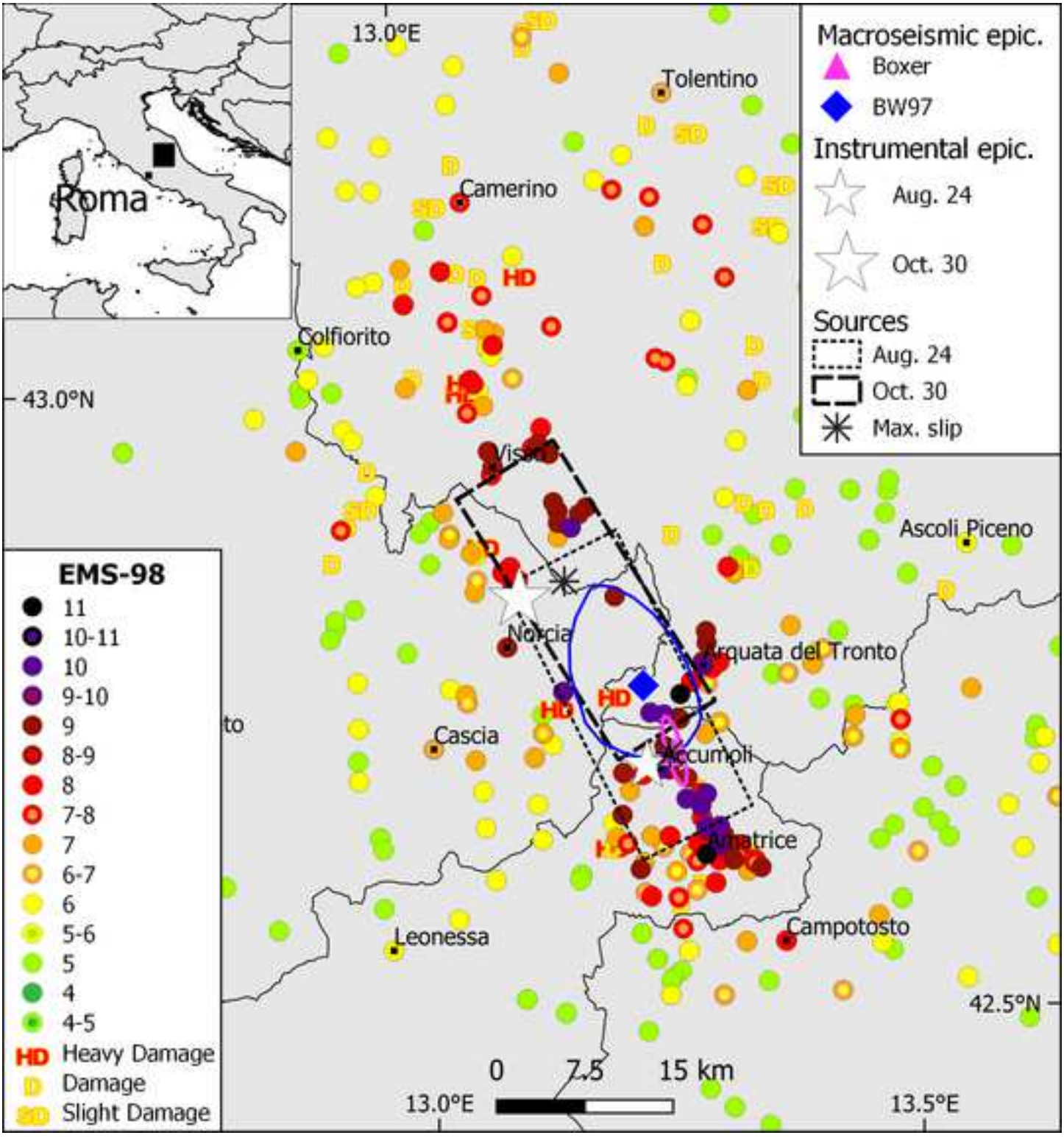

Figure

Click here to access/download;Figure;Fig5.jpg

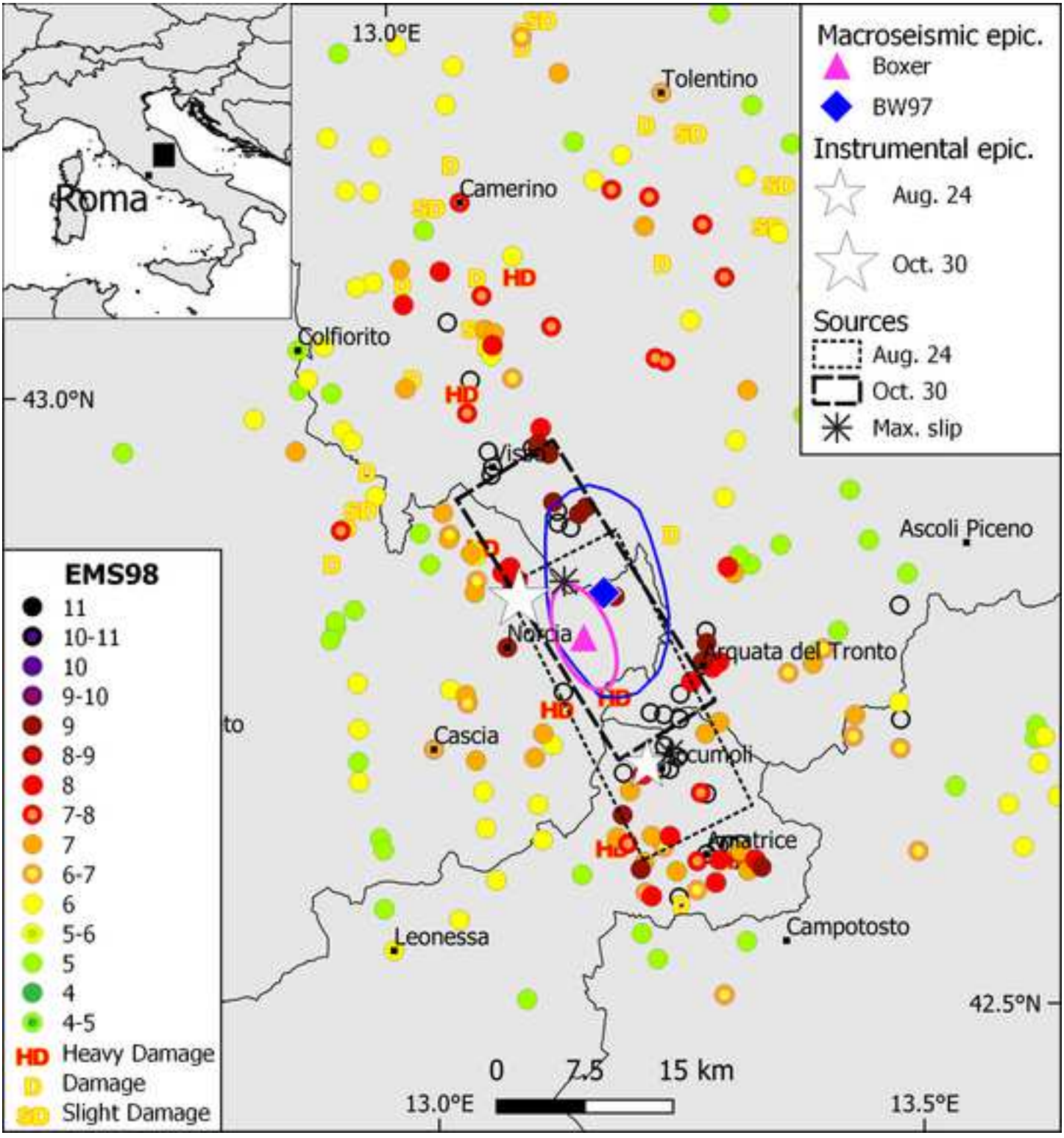

Figure

Click here to access/download;Figure;Fig6.jpg

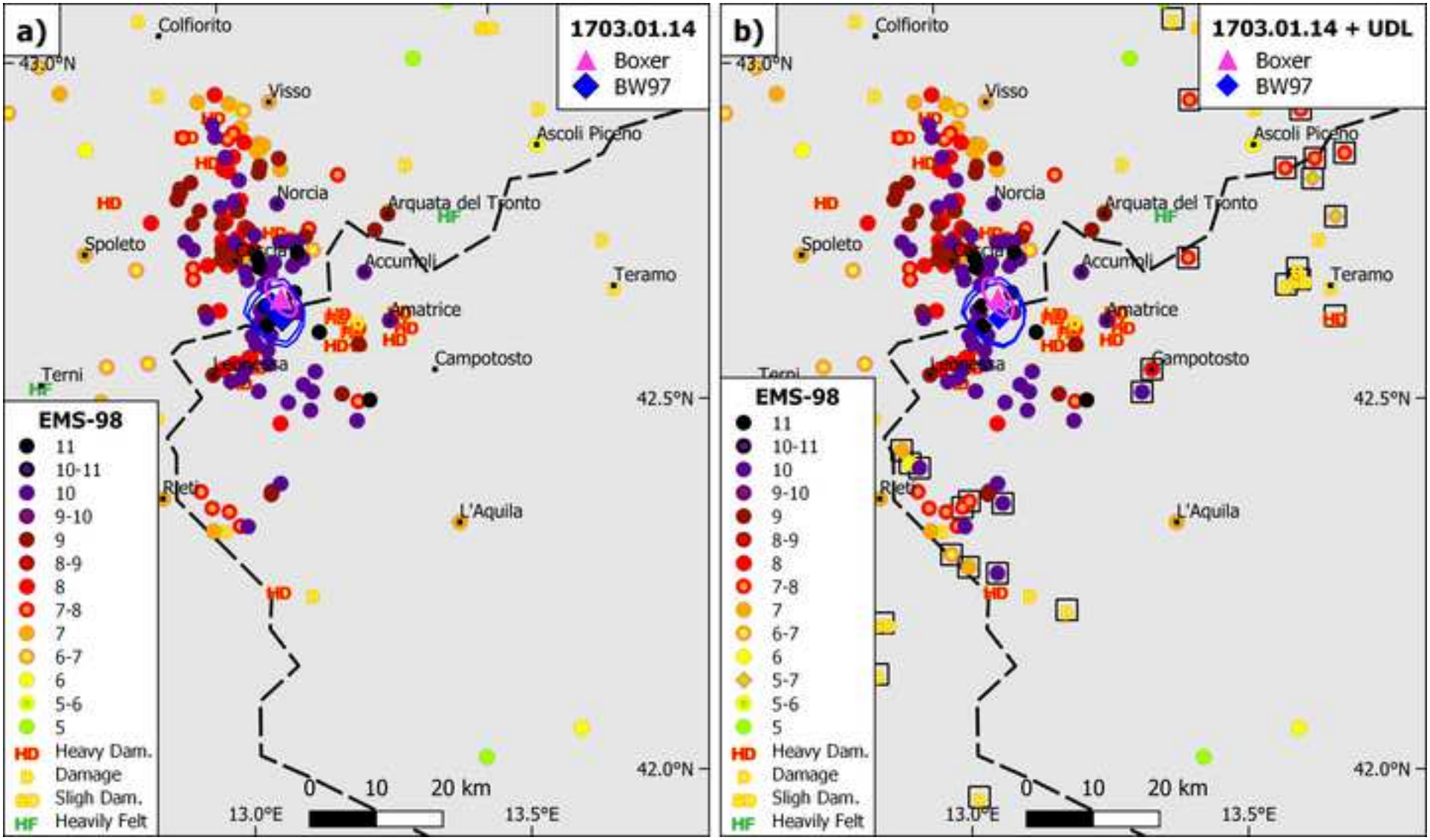

Figure

Click here to access/download;Figure;Fig7.jpg

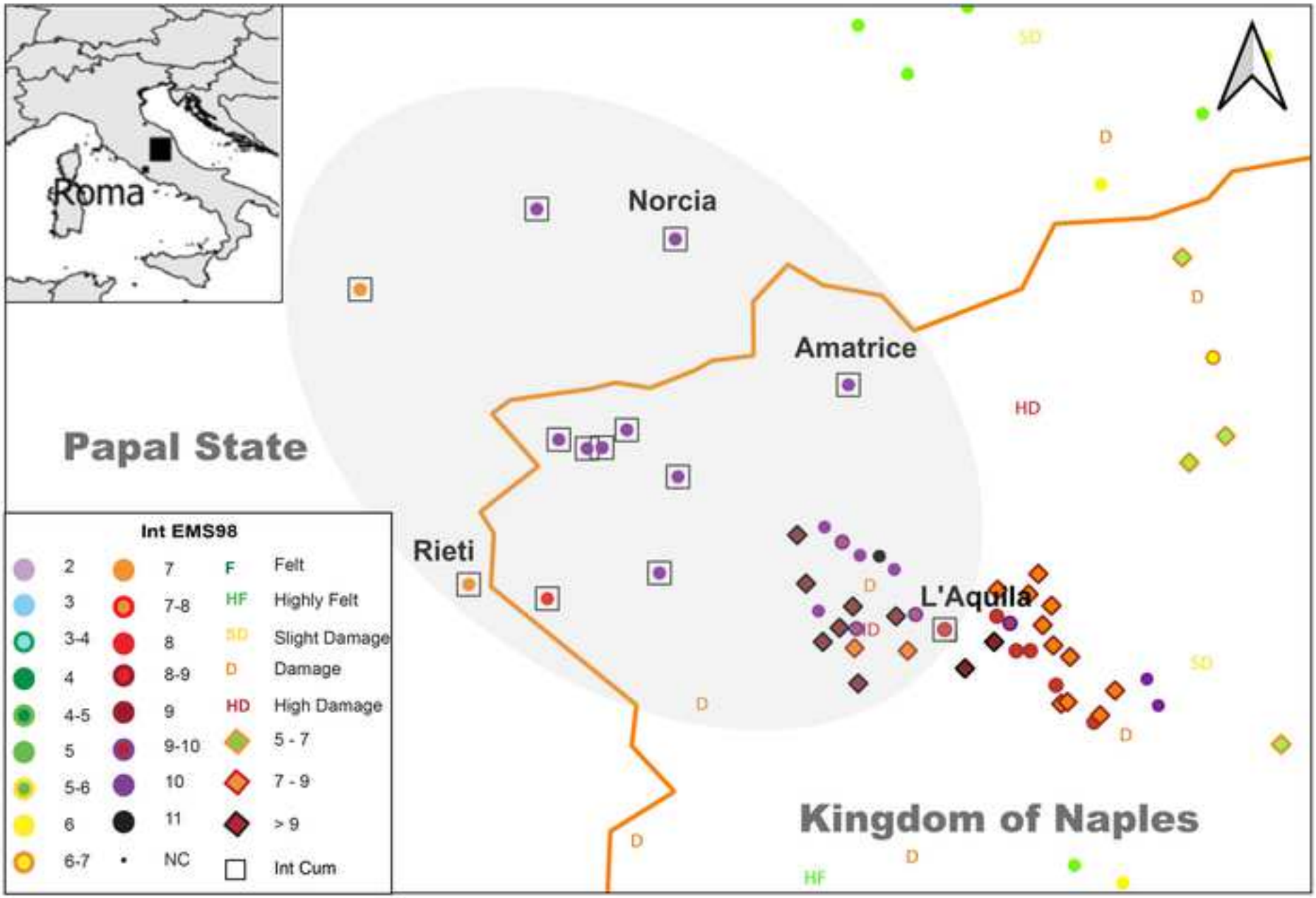

Figure

Click here to access/download;Figure;Fig8A.jpg

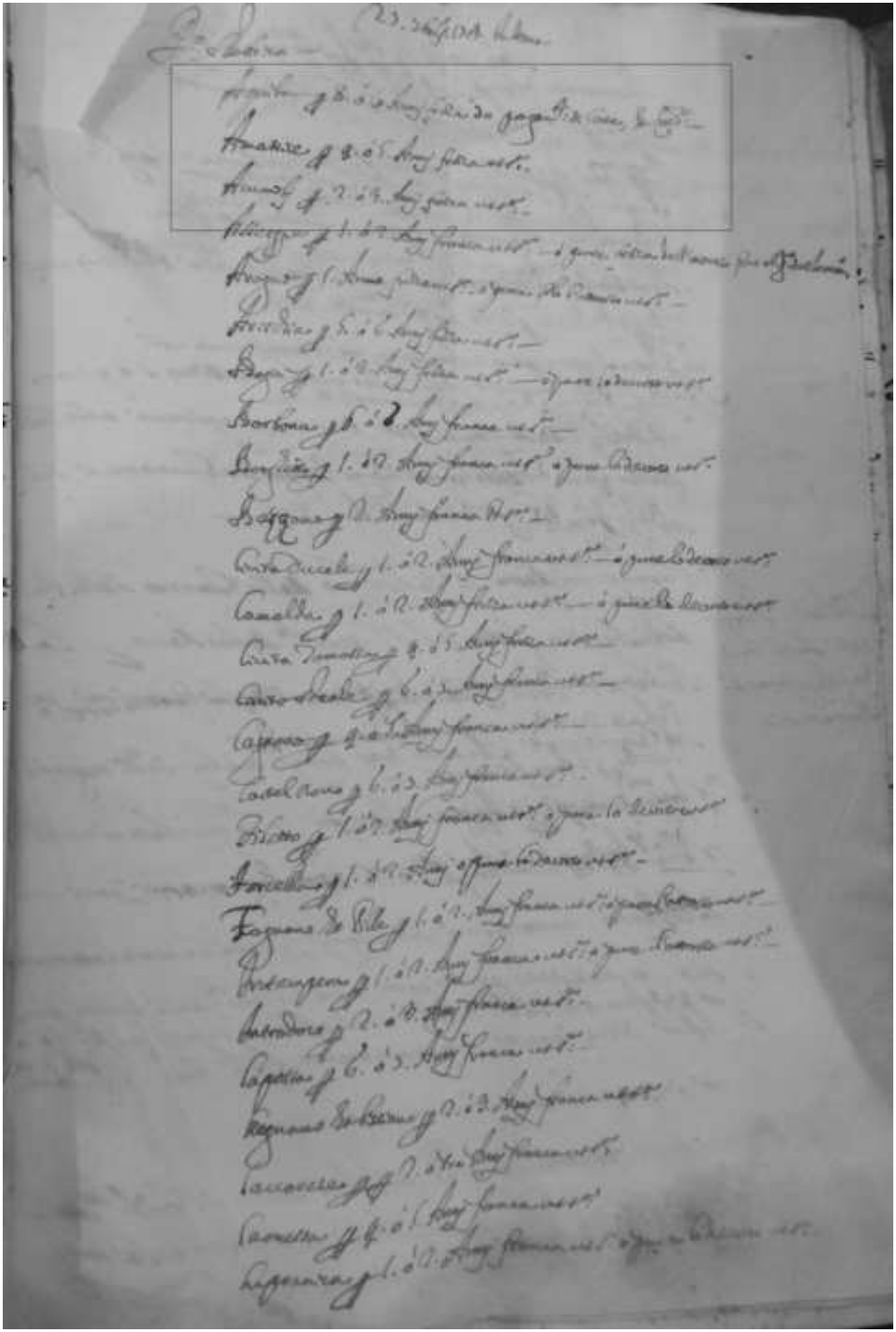

Figure

Click here to access/download;Figure;Fig8B.jpg

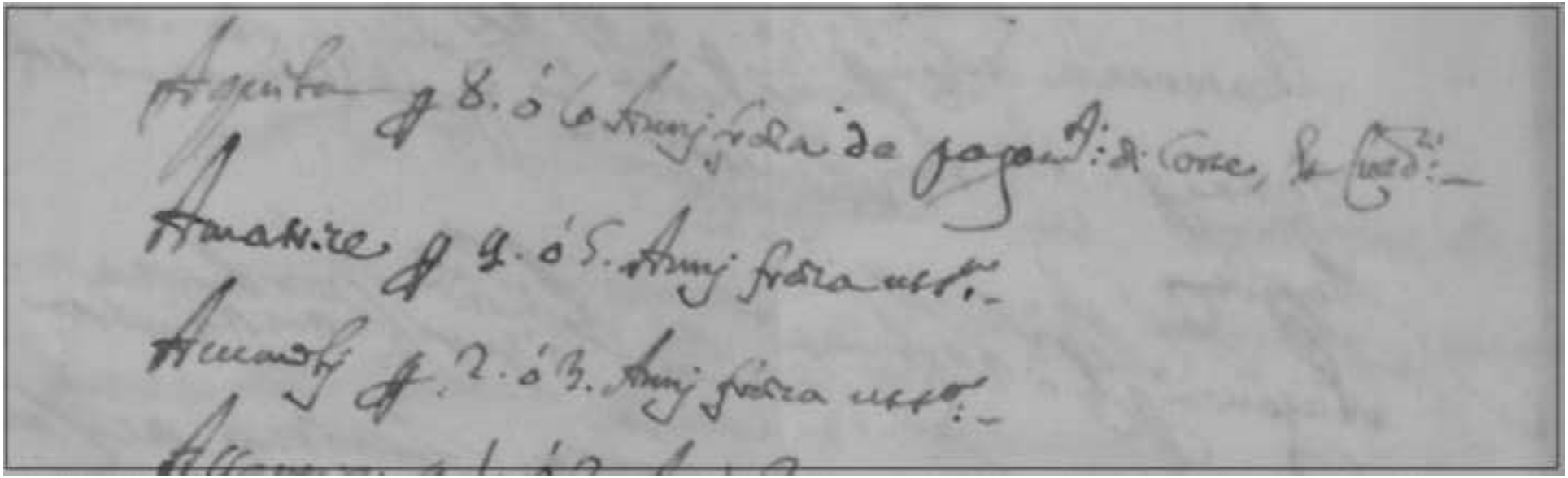

Figure

Click here to access/download;Figure;Fig9.jpg

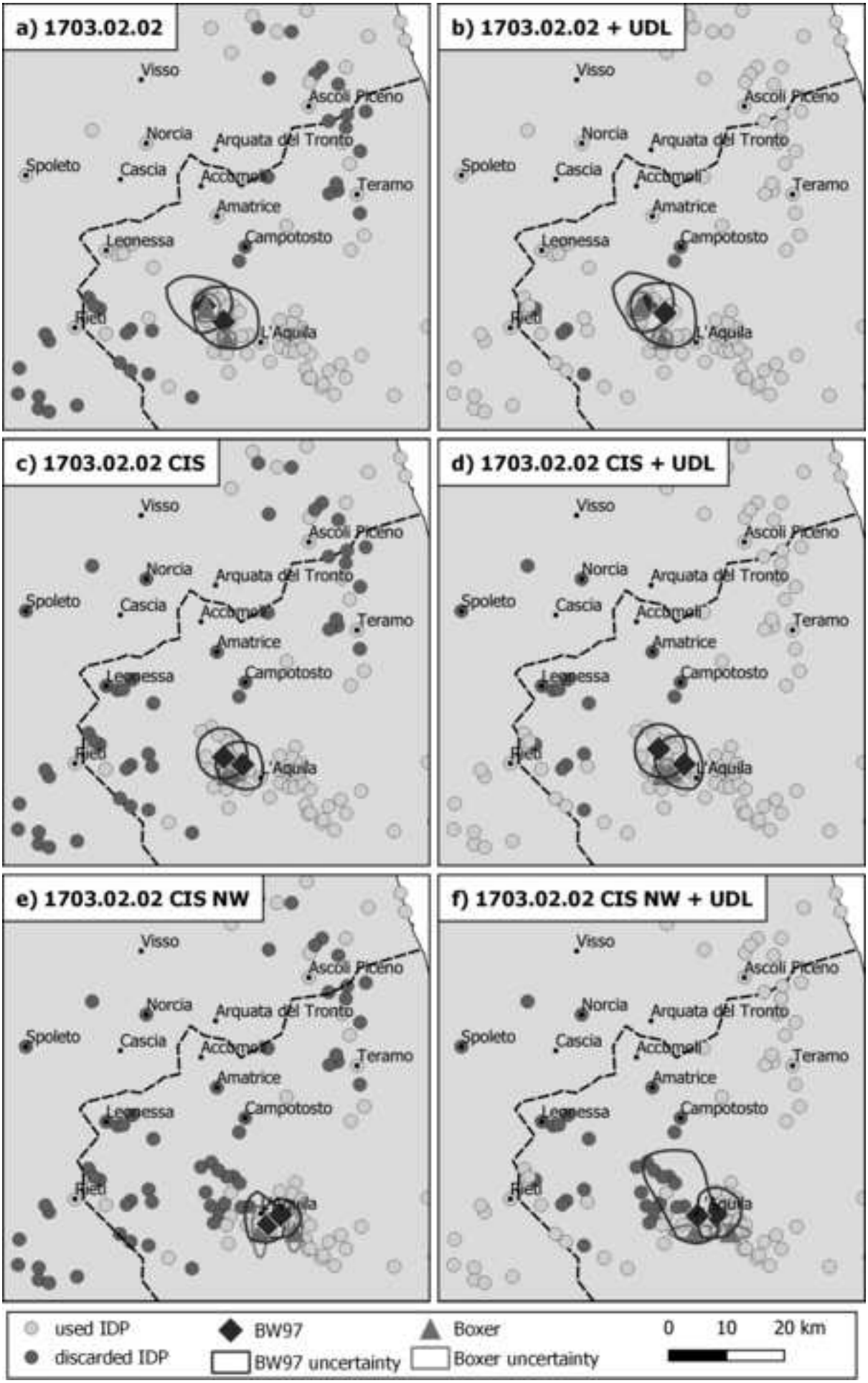

Figure

Click here to access/download;Figure;Fig10.jpg

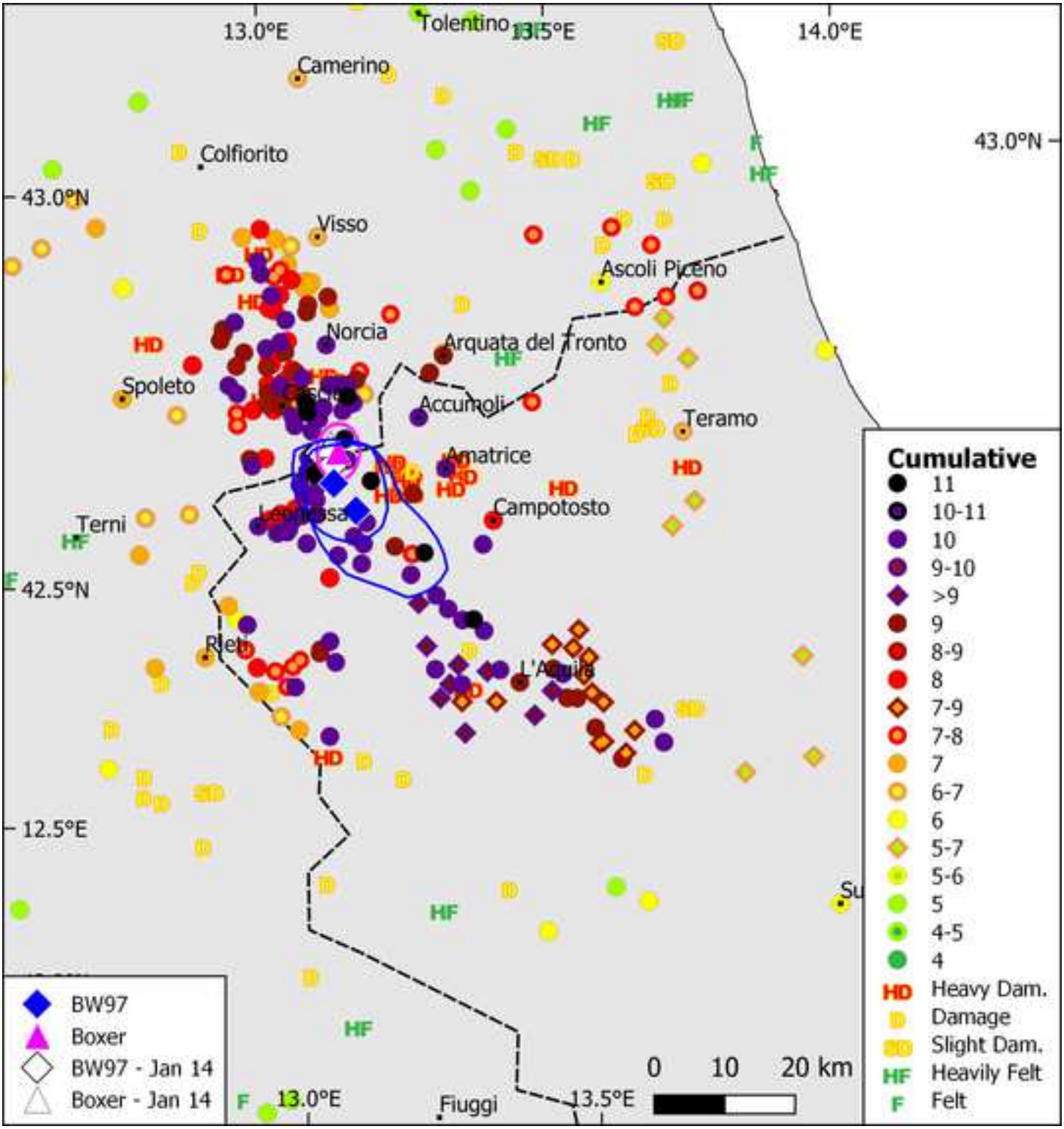

Figure

Click here to access/download;Figure;Fig11.jpg